EFFECT OF BASE STATION HEIGHT ON CHANNEL MODELING IN 5G COMMUNICATIONS

M.M. Prasada Reddy

Professor, Dept of E.C.E, NCET, Hyderabad, India, 500070.
Email - maruthiprasadareddy@gmail.com

Abstract: *This paper describes cannel responses of Urban Micro cell* (UMi) *at different base station heights to design fifth generation* $(5G)$ *mobile and cellular communications using* $NYUSIM$. $NYUSIM$ *is based on statistical spatial channel model for broad band millimeter wave (mm Wave) wireless communication systems.* $NYUSIM$ *is suitable for wide range of carrier frequencies from* $0.5\ GHz\ to\ 100\ GHz, RF$ *band width from* $0\ to\ 800\ MHz$*, antenna beam width is in the range of* $7^0\ to\ 360^0$ *for azimuth and* $7^0\ to\ 45^0$ *for elevation*

Key Words: $NYUSIM$, *Channel model,* $mm\ Wave$,$5G, UMA, UMi, RMa$.

1. INTRODUCTION :

The design and implementation of channel models are very crucial for wireless communication system design. Channel simulators play a key role for performance analysis of communication system. Many channel simulators have already been well studied in the past[1]-[7].

Name of the simulator designer	purpose
Smith[1]	Developed a simulation tool for indoor and outdoor propagation channel, using two ray Rayleigh fading cannel model, modeled by Clarke [9].
Fraun hofer Heinrich hertz institute [2]	Developed $3D$ multi channel model, that predicts the performance of an UMa
[3]	Developed for indoor scenarios, which is suitable for machine to machine applications
Rappaport and Scidel [4]	Developed statistical indoor channel model, that is, SIRCIM (simulation of indoor Radio Channel Impulse response Model).Operating range 10 MHz to 60 GHz
[5],[6]	Developed simulation of mobile radio channel impulse response model (SMRCIM),that is used for simulating outdoor channels
Fung et al [7]	Developed BERSIM to simulate mobile radio communications and to estimate average Bit Error Rate .Using BERSIM link quality can be evaluated in real time without using any RF hardware.

Table 1: Literature Survey

In this paper, NYUSIM [10] is introduced which is a open source channel simulator ,used at multi meter wave (mm Wave) frequencies (28 to 73 GHz) in different outdoor environments like UMi,UMa and RMa environments [11]-[19].This simulator provides accurate channel impulse responses in both time and space. NYUSIM supports carrier frequencies in the range 0.5 GHZ-100GHz and Radio frequency band widths in the range 0 to 800 MHz. The source code is developed in MATLAB[20].NYUSIM works on Windows or Macintosh operating system even without installing MATLAB.

2 CHANNEL MODEL SUPPORTED BY NYUSIM

Omni directional channel models are well adopted across the globe in designing wireless system. But directional channel models are very important to design and implement antenna arrays to spatial uniformity and beam forming gain Multi path Input Multipath Output (MIMO) system[21][22].NYUSIM generates Channel Impulse Responses (CIR) for both Omni directional and directional channel models [10]-[19].The main advantage of NYUSIM is that it generates functions of spatial and temporal CIRs. This section describes the path loss (PL) model used in NYUSIM.

PATH LOSS MODEL AND CLUSTERING DEFINITION IN NYUSIM

A. PATH LOSS MODEL

The Close In free space reference distance (CI) path loss model with a $1m$ reference distance[12],[15],[17],[19] and an extra attenuation due to various atmospheric conditions [23],is employed in NYUSIM, which is expressed as [12],[15],[24].

$PL^{CI}(\mathrm{f,d})[\mathrm{dB}] = \mathrm{FSPL(f,1m)[dB]} + 10\mathrm{n}\log 10^{\mathrm{d}} + \mathrm{AT[dB]} + \mathrm{X}_{\sigma}^{\mathrm{CI}} \ldots\ldots\ldots\ldots (1)$

where

$d \geq 1m$

f = carrier frequency in GHz

d = 3D T-R separation distance.

n =Path Loss Exponent (PLE)

AT= Attenuation term induced by the atmosphere

$\mathrm{X}_{\sigma}^{\mathrm{CI}}$ = Zero mean random Gaussian variable with a standard deviation σ in dB

FSPL(f, 1m) = Free space path loss in dB at a T-R separation distance of $1m$at a carrier frequency f

$\mathrm{FSPL(f,1m)[dB]} = 20\log 10^{\left(\frac{4\pi \mathrm{f}\times 10^{9}}{\mathrm{c}}\right)} = 32.4\ \mathrm{dB} + 20\log 10^{\mathrm{f}} \ldots\ldots\ldots\ldots\ldots (2)$

where c = speed of light

f = carrier frequency in GHz and

$\mathrm{AT[dB]} = \alpha[\mathrm{dB/m}] \times \mathrm{d(m)} \ldots\ldots\ldots\ldots\ldots\ldots\ldots\ldots\ldots (3)$

where α =attenuation factor in dB/m [1GHz to 100 GHz] which includes, collective attenuation effects of dry air (including oxygen),water vapor rain and haze[23].

$\mathrm{d} = 3\mathrm{D\ T} - \mathrm{R}$ separation distance [1].

Figure 1 provides better insight into on propagation attenuation values due to dry air, vapor, haze and rain at mm Wave frequencies (1GHZ to 100 GHz),with a barometric pressure of 1013.25 m bar, a relative humidity of 50%, a temperature of 20^0C and a rain rate of 5 mm/hr [23].

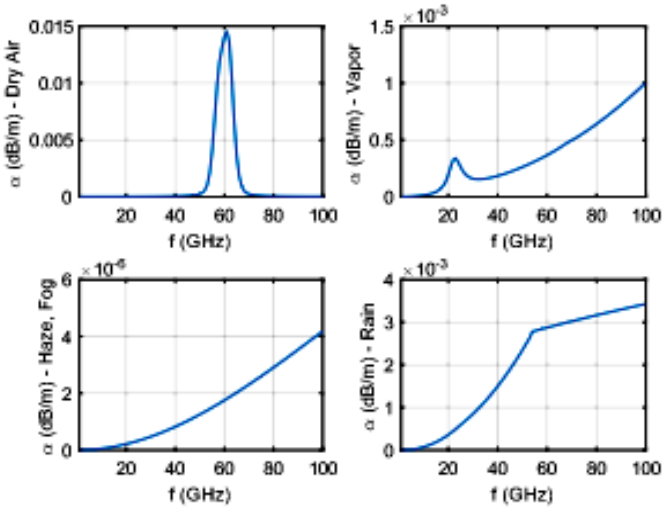

Fig. 1: Propagation attenuation due to dry air, vapor, haze, and rain at mmWave frequencies, with a barometric pressure of 1013.25 mbar, a relative humidity of 80%, a temperature of 20◦C, and a rain rate of 5 mm/hr [23].

B. CLUSTERING DEFINITION IN NYUSIM:

NYUSIM uses time cluster (TC) and spatial lobe (SL) concepts to describe multipath behavior in Omni directional channel impulse responses (CIRs). TCs are composed of multipath components traveling close in time, and arriving from potentially different directions in a short propagation time window. SLs denote primary directions of departure (or arrival) where energy arrives over several hundred nanoseconds [6]. Per the definitions given above, a TC contains multipath components traveling close in time, but may arrive from different SL angular directions, such that the temporal and spatial statistics are decoupled and can be recovered separately. Similarly, an SL may contain many multipath components arriving (or departing) in a space (angular cluster) but with different time delays. This distinguishing feature is obtained from realworld propagation measurements [1], [5] which have shown that multipath components belonging to the same TC can arrive at distinct spatial pointing angles and that energy arriving or departing in a particular pointing direction can span hundreds or thousands of nanoseconds in propagation delay, detectable due to high-gain rotatable directional antennas. The TCSL clustering scheme is physically based, for instance, it utilizes a fixed intercluster void interval to represent the minimum propagation time between possible obstructions causing reflection, scattering, or diffraction, and is derived from field observations based on about 1 Tb of measured data over many years, and can be used to extract TC and SL statistics for any measurement or ray-tracing data sets [6].

3. GUI AND SIMULATOR BASICS

The screen shot in figure 2 illustrates the GUI of NYUSIM.NYUSIM performs Monte Carlo simulations, generates certain number of samples of CIRs at a specific T-R separation distance. The number of samples and T-R separation distances are to be given by the user.

A .INPUT PARAMETERS

There are 28 input parameters on GUI of NYUSIM. They are divided into two categories: Channel parameters and Antenna parameters. Channel parameters consists of 16 basic input parameters related to propagation channel and antenna properties consists of 12 input parameters about the Tx and Rx antenna arrays.

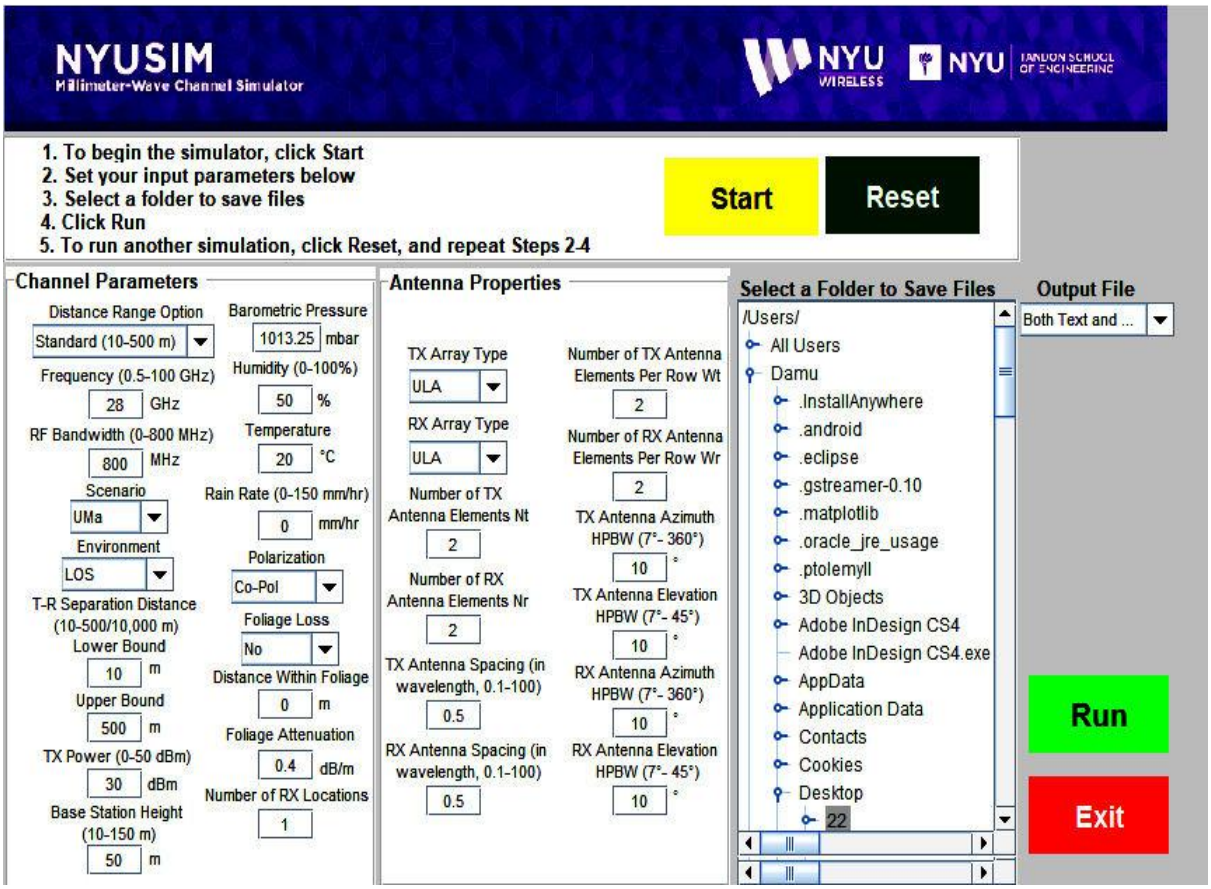

Fig. 2: Graphical User Interface (GUI) of the NYUSIM channel model simulator

B. OUTPUT FILES

In each simulation run 6 figures are generated. The six output figures are

- 3D AOD power spectrum
- 3D AOA power spectrum
- A sample of Omni directional power delay profile (PDP)
- A sample of directional PDP with strongest power
- A series of PDPs over different receive antenna elements
- Path Loss scattering plot

Figure 5 shows the path loss (directional and Omni directional)scatter plot generated after N simulation runs over the entire distance along with the fixed PLE and fading standard deviation using the minimum mean square error (MMSE) technique [15],[17].In the legend of figure 5

n: represents PLE
σ: shadow fading standard deviation
Omni : Omni directional
dir : directional
dir-best: direction with strongest received power

To produce directional path loss at each Rx location .NYUSIM searches for all possible pointing angles in increments of azimuth and elevation of HPBWs of the Tx/Rx antenna specified by the user on GUI after first generating the Omni directional PDP. The TX/Rx antenna gain pattern is calculated by NYUSIM using equations (45) and (46) in [13] based on Azimuth and elevation HPBWs of Tx and Rx antennas as mentioned by the user on GUI

Directional path loss(DPL) =Tx power +Tx and Rx antenna gain −directional received power [11],[12]. DPL and DPLE will always be larger (because directional channel is always lossy) than Omni directional , because, the directional antenna will spatially filter out many MPCs due to its directional pattern ,then Rx receives fewer MPCs hence less energy, so the directional path loss is higher after removing the antenna gain effect from the received power [12],[17].

C. OUTPUT DATA FILES

For each simulation run, five sets of .txt files and five corresponding .mat files are generated, namely, "AODLobePowerSpectrumn Lobex.txt", "AODLobePowerSpectrumn.mat", "AOALobePowerSpectrumn Lobex.txt", "AOALobePowerSpectrumn.mat", "OmniPDPn.txt", "OmniPDPn.mat", "DirectionalPDPn.txt", "DirectionalPDPn.mat", "SmallScalePDPn.txt", and "SmallScalePDPn.mat", where n denotes the nth RX location (i.e., nth simulation run), and x represents the xth spatial lobe. After N continuous simulation runs, another three .txt files and three corresponding .mat files are produced, i.e., "BasicParameters.txt", "BasicParameters.mat", "OmniPDPInfo.txt", "OmniPDPInfo.mat", "DirPDPInfo.txt", and "DirPDPInfo.mat". The files "BasicParameters.txt" and "BasicParameters.mat" subsume all the input parameter values as shown on the GUI when running the simulation. The files "OmniPDPInfo.txt" and "OmniPDPInfo.mat" contain four columns where each column represents a key parameter for each of the N omnidirectional PDPs from N continuous simulation runs, including T-R separation distance, omnidirectional received power, omnidirectional path loss, and omnidirectional root-meansquare (RMS) delay spread. The files "DirPDPInfo.txt" and "DirPDPInfo.mat" contain 10 columns where each column represents a key parameter for each of the directional PDPs from N continuous simulation runs, such as time delay, received power, phase, azimuth and elevation AODs and AOAs of each resolvable MPC (i.e., antenna pointing angle), along with directional path loss and directional RMS delay spread. Each "AOD Lobe Power Spectrumn Lobex" file is associated with a corresponding 3D AOD power spectrum output figure, and contains five parameters (columns) of each resolvable MPC in an AOD spatial lobe, namely: pathDelay (ns), path Power (mWatts), path Phase (rad), AOD (degree), and ZOD (degree). Similar parameters are contained in each .txt and .mat file "AOA Lobe Power Spectrumn Lobe x" that is associated with the output figure of 3D AOA power spectrum.

Each "OmniPDPn" file is associated with an omnidirectional PDP output figure, and contains two columns: the first column denotes the propagation time delay in nanoseconds, and the second column represents the received power in dBm. Each .txt and .mat file "DirectionalPDPn" is associated with the output figure of directional PDP with strongest power, and contains two columns: the first column denotes the propagation time delay in nanoseconds, and the second column represents the received power in dBm. Each .txt and .mat file "SmallScalePDPn" is associated with the output figure of the series of omnidirectional PDPs over different RX antenna elements, and contains three columns: the RX antenna separation in terms of number of wavelengths, the propagation time delay in nanoseconds, and the received power in dBm.

4. RESULTS :

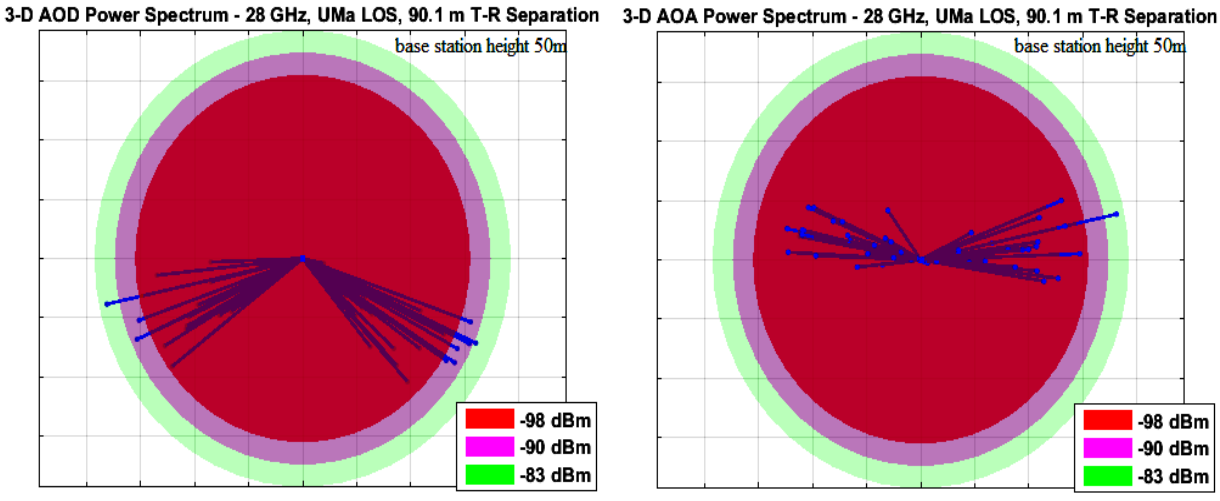

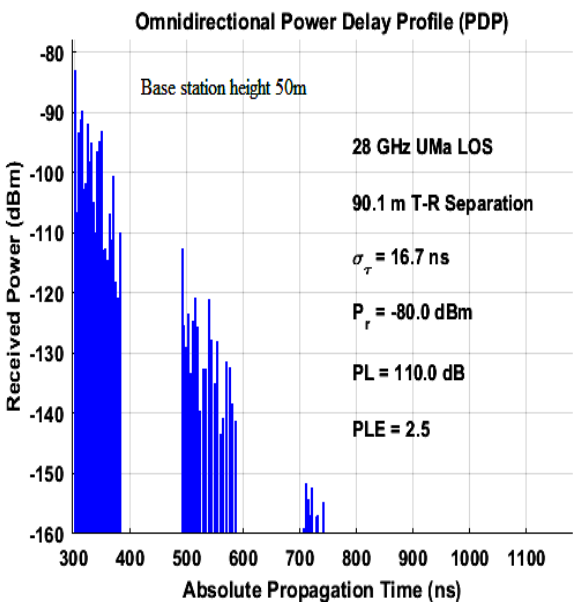
Omnidirectional Power Delay Profile (PDP)
Base station height 50m
28 GHz UMa LOS
90.1 m T-R Separation
σ_τ = 16.7 ns
P_r = -80.0 dBm
PL = 110.0 dB
PLE = 2.5
Received Power (dBm)
Absolute Propagation Time (ns)

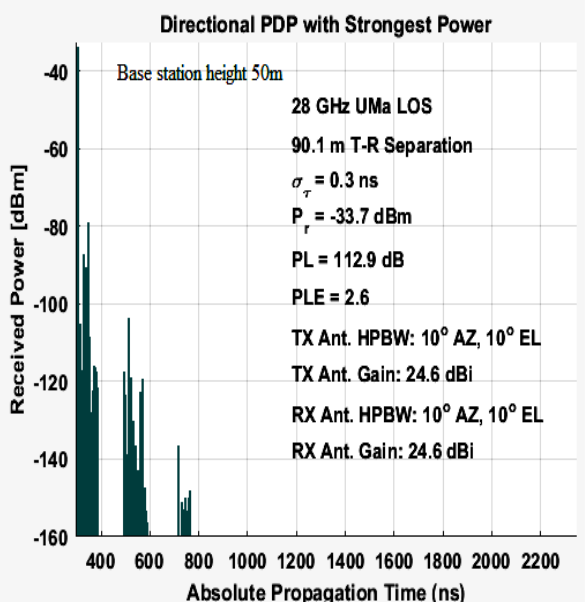
Directional PDP with Strongest Power
Base station height 50m
28 GHz UMa LOS
90.1 m T-R Separation
σ_τ = 0.3 ns
P_r = -33.7 dBm
PL = 112.9 dB
PLE = 2.6
TX Ant. HPBW: 10° AZ, 10° EL
TX Ant. Gain: 24.6 dBi
RX Ant. HPBW: 10° AZ, 10° EL
RX Ant. Gain: 24.6 dBi
Received Power [dBm]
Absolute Propagation Time (ns)

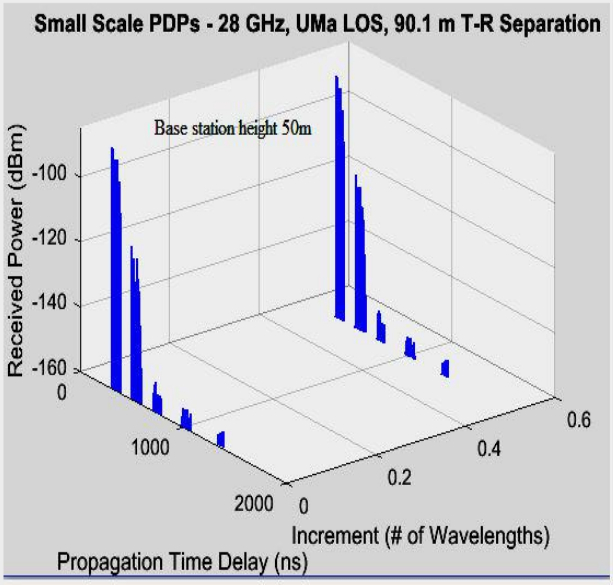
Small Scale PDPs - 28 GHz, UMa LOS, 90.1 m T-R Separation
Base station height 50m
Received Power (dBm)
Propagation Time Delay (ns)
Increment (# of Wavelengths)

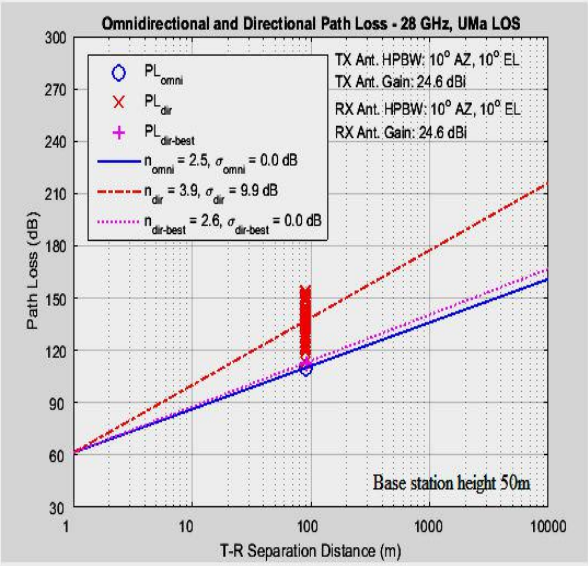
Omnidirectional and Directional Path Loss - 28 GHz, UMa LOS
PL_{omni}
PL_{dir}
$PL_{dir-best}$
n_{omni} = 2.5, σ_{omni} = 0.0 dB
n_{dir} = 3.9, σ_{dir} = 9.9 dB
$n_{dir-best}$ = 2.6, $\sigma_{dir-best}$ = 0.0 dB
TX Ant. HPBW: 10° AZ, 10° EL
TX Ant. Gain: 24.6 dBi
RX Ant. HPBW: 10° AZ, 10° EL
RX Ant. Gain: 24.6 dBi
Base station height 50m
Path Loss (dB)
T-R Separation Distance (m)

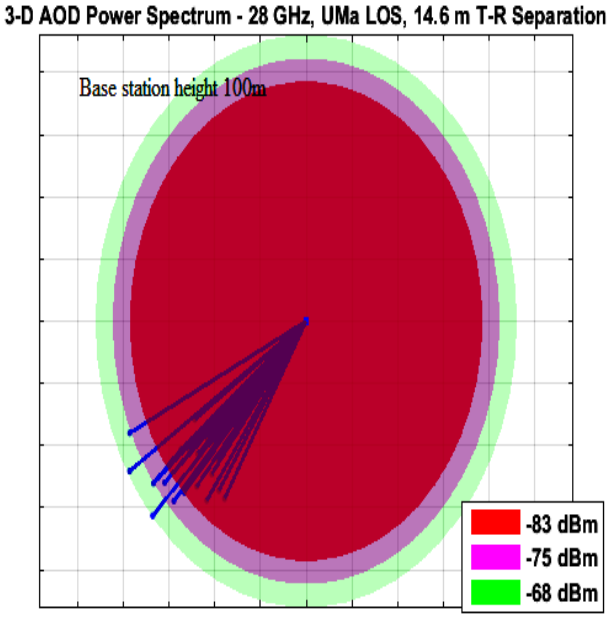
3-D AOD Power Spectrum - 28 GHz, UMa LOS, 14.6 m T-R Separation
Base station height 100m
-83 dBm
-75 dBm
-68 dBm

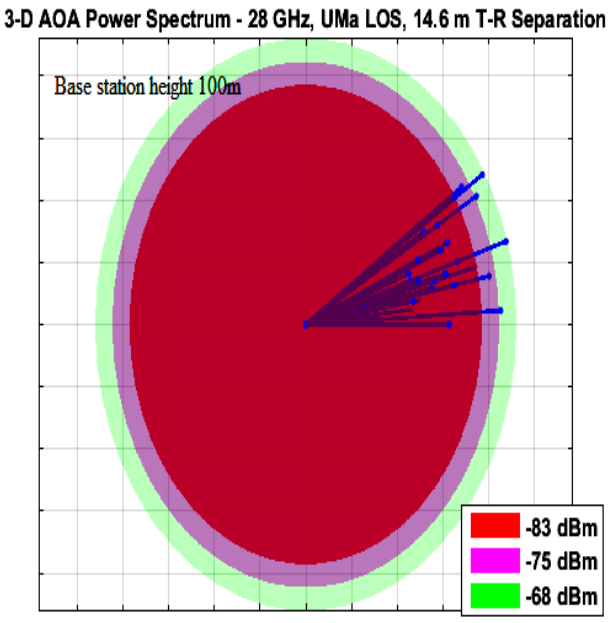
3-D AOA Power Spectrum - 28 GHz, UMa LOS, 14.6 m T-R Separation
Base station height 100m
-83 dBm
-75 dBm
-68 dBm

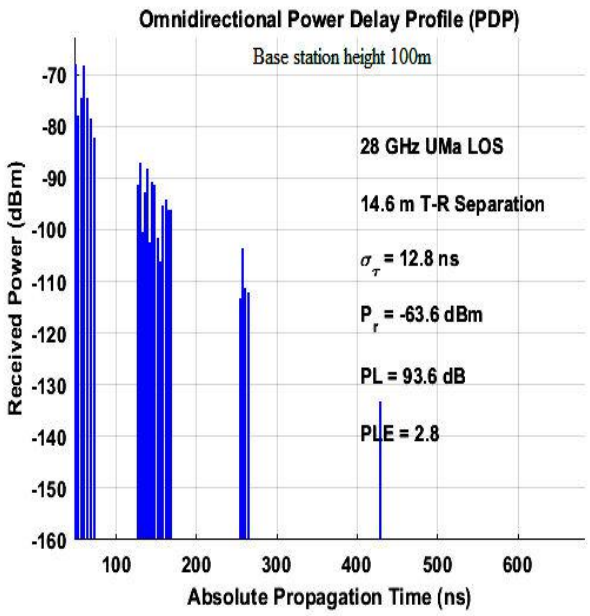
Omnidirectional Power Delay Profile (PDP)
Base station height 100m
28 GHz UMa LOS
14.6 m T-R Separation
σ_τ = 12.8 ns
P_r = -63.6 dBm
PL = 93.6 dB
PLE = 2.8
Received Power (dBm)
Absolute Propagation Time (ns)

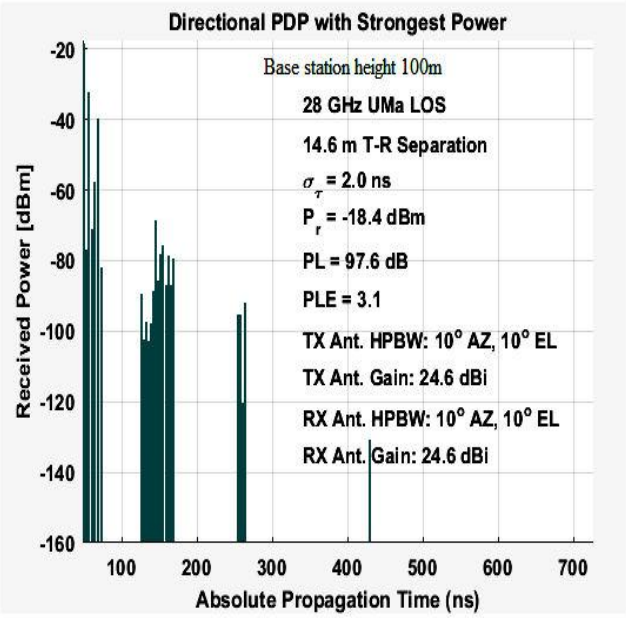
Directional PDP with Strongest Power
Base station height 100m
28 GHz UMa LOS
14.6 m T-R Separation
σ_τ = 2.0 ns
P_r = -18.4 dBm
PL = 97.6 dB
PLE = 3.1
TX Ant. HPBW: 10° AZ, 10° EL
TX Ant. Gain: 24.6 dBi
RX Ant. HPBW: 10° AZ, 10° EL
RX Ant. Gain: 24.6 dBi
Received Power [dBm]
Absolute Propagation Time (ns)

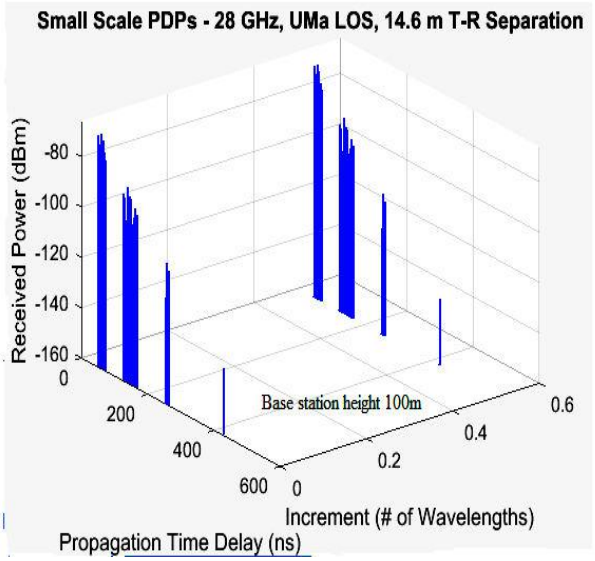
Small Scale PDPs - 28 GHz, UMa LOS, 14.6 m T-R Separation
Base station height 100m
Received Power (dBm)
Propagation Time Delay (ns)
Increment (# of Wavelengths)

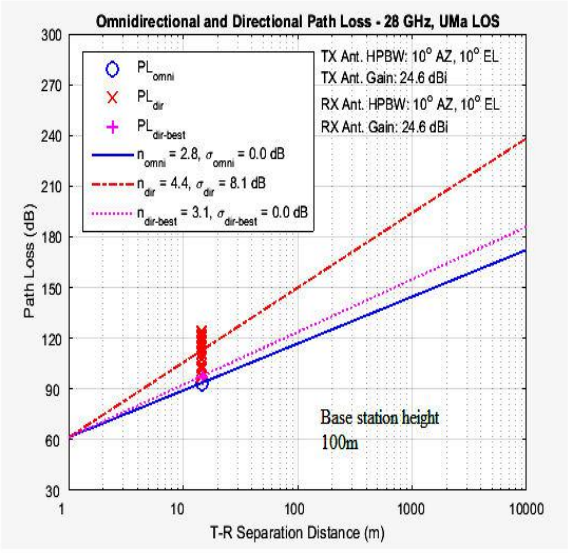
Omnidirectional and Directional Path Loss - 28 GHz, UMa LOS
PL_{omni}
PL_{dir}
$PL_{dir-best}$
n_{omni} = 2.8, σ_{omni} = 0.0 dB
n_{dir} = 4.4, σ_{dir} = 8.1 dB
$n_{dir-best}$ = 3.1, $\sigma_{dir-best}$ = 0.0 dB
TX Ant. HPBW: 10° AZ, 10° EL
TX Ant. Gain: 24.6 dBi
RX Ant. HPBW: 10° AZ, 10° EL
RX Ant. Gain: 24.6 dBi
Base station height 100m
Path Loss (dB)
T-R Separation Distance (m)

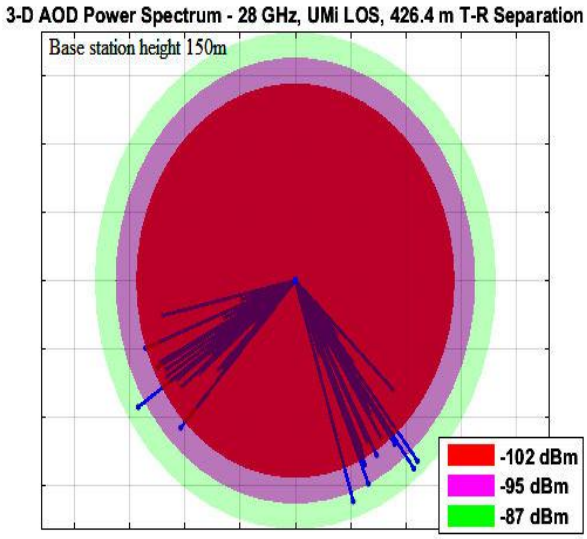
3-D AOD Power Spectrum - 28 GHz, UMi LOS, 426.4 m T-R Separation
Base station height 150m
-102 dBm
-95 dBm
-87 dBm

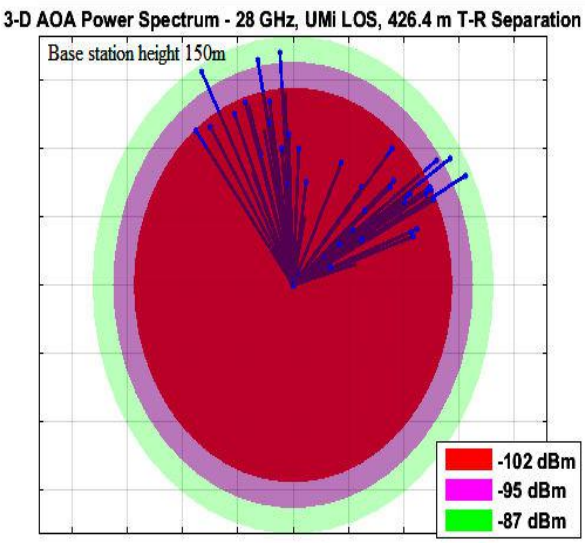
3-D AOA Power Spectrum - 28 GHz, UMi LOS, 426.4 m T-R Separation
Base station height 150m
-102 dBm
-95 dBm
-87 dBm

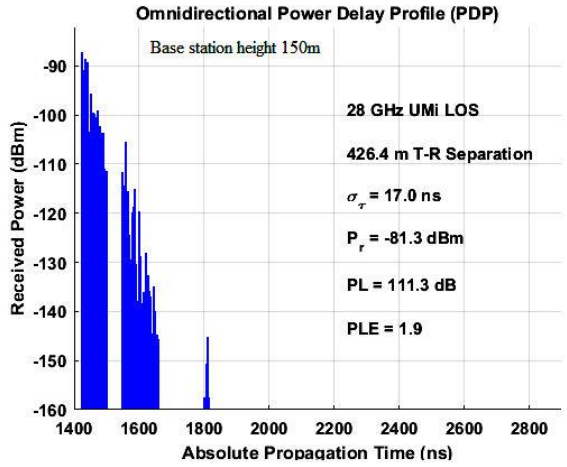

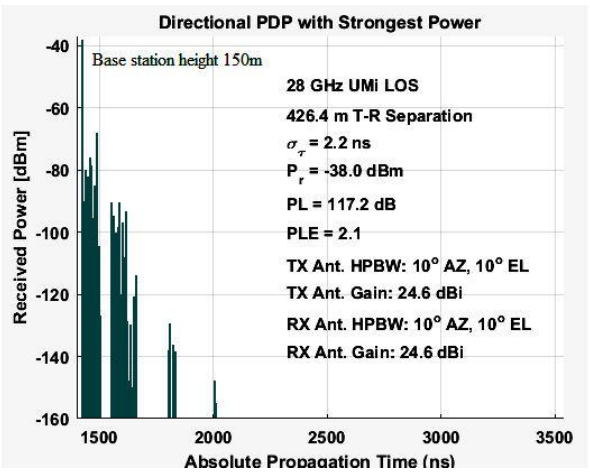

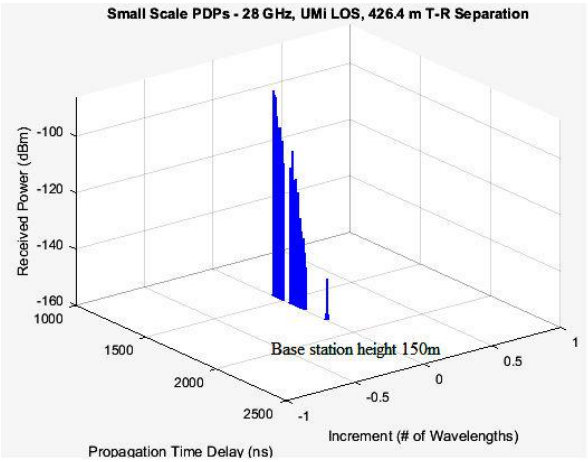

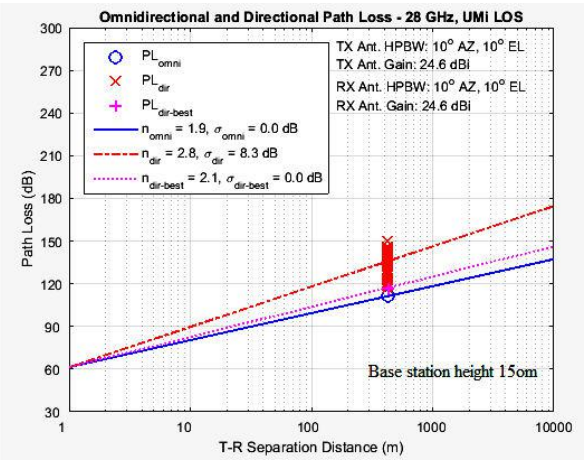

Table -1: Omni directional PDP at different base station heights

	Base station height 50m	Base station height 100m	Base station height 150m
σ_T	21.6 ns	12.8 ns	17 ns
P_R	-77 dBm	-63.6 dBm	-81.3 dBm
P_L	107 dB	93.6 dB	111.3 dB
PLE	1.9	2.8	1.9
T-R separation	90.1m	14.6m	426.4m

Table 2: Directional PDP with strongest power

	Base station height 50m	Base station height 100m	Base station height 150m
σ_T	0.3 ns	2 ns	2.2 ns
P_R	-33.7 dBm	-18.4 dBm	-38 dBm
P_L	112.9 dB	97.6 dB	17.2 dB
PLE	2.6	3.1	2.1
T-R separation	90.1m	14.6m	426.4m
Tx Gain	24.6dBi	24.6dBi	24.6dBi
Rx Gain	24.6dBi	24.6dBi	24.6dBi

Table 3: Omni directional and directional path loss at different base station heights

BS height	n_{omni}	σ_{omni}	n_{dir}	σ_{dir}	$n_{dir-best}$	$\sigma_{dir-best}$
50m	2.5	0 dB	3.9	9.9 dB	2.6	0 dB
100m	2.8	0 dB	4.4	8.1 dB	3.1	0 dB
150m	1.9	0 dB	2.8	8.3 dB	2.1	0 dB

5. APPLICATIONS OF NYUSIM:

The output figures and data files generated from NYUSIM can be used to simulate CIRs for mm Wave system to investigate MIMO channel performance and to perform BER simulations[7],[33].Using NYUSIM the condition number of a MIMO channel can be obtained as discussed in [41]

Condition-number measurements are an excellent engineering tool for several reasons:

- They effectively measure MIMO operation by combining the effects of noise and undesirable channel correlation.
- They are measured directly from channel frequency response, without the need for demodulation or a matrix decoder.
- They are a frequency- or subcarrier-specific measurement, useful for uncovering frequency response effects.
- They relate a somewhat abstract matrix characteristic to practical RF signal characteristics such as SNR.

6. CONCLUSION:

This paper describes an open source channel simulator (NYUSIM), used for broad band propagation measurements at mm Wave frequencies. NYUSIM generates wideband PDPs/CIRs channel statistics for different base station heights in Urban Micro Cell (UMi) environment.

REFERENCES:

1. S. Y. Seidel, K. Takamizawa, and T. S. Rappaport,(May 1989) “Application of second-order statistics for an indoor radio channel model,” in IEEE 39th Vehicular Technology Conference, pp. 888–892 vol.2.
2. S. Jaeckel et al.(June 2014), “QuaDRiGa: A 3-D multi-cell channel model with time evolution for enabling virtual field trials,” IEEE Transactions on Antennas and Propagation, vol. 62, no. 6, pp. 3242–3256,.
3. Y. Yu et al.(Dec. 2015), “Propagation model and channel simulator under indoor stair environment for machine-to-machine applications,” in 2015 AsiaPacific Microwave Conference, vol. 2, , pp. 1–3.
4. T. S. Rappaport et al.(May 1991), “Statistical channel impulse response models for factory and open plan building radio communicate system design,” IEEE Transactions on Communications, vol. 39, no. 5, pp. 794–807,.
5. Wireless Valley Communications, Inc., SMRCIM Plus 4.0 (Simulation of Mobile Radio Channel Impulse Response Models) Users Manual, Aug. 1999.
6. V. K. Rajendran et al., “Concepts and implementation of a semantic web archiving and simulation system for rf propagation measurements,” in 2011 IEEE Vehicular Technology Conference (VTC Fall), Sept 2011, pp. 1–5.
7. V. Fung et al., “Bit error simulation for pi/4 DQPSK mobile radio communications using two-ray and measurement-based impulse response models,” IEEE Journal on Selected Areas in Communications, vol. 11, no. 3, pp. 393–405, Apr. 1993.
8. J. I. Smith, “A computer generated multipath fading simulation for mobile radio,” IEEE Transactions on Vehicular Technology, vol. 24, no. 3, pp. 39–40, Aug 1975.
9. R. H. Clarke, “A statistical theory of mobile-radio reception,” The Bell System Technical Journal, vol. 47, no. 6, pp. 957–1000, July 1968.
10. New York University, NYUSIM, 2016. [Online]. Available: http://wireless.engineering.nyu.edu/5gmillimeter-wave-channelmodeling-software/.
11. T. S. Rappaport et al., “Millimeter wave mobile communications for 5G cellular: It will work!” IEEE Access, vol. 1, pp. 335– 349, 2013.
12. “Wideband millimeter-wave propagation measurements and channel models for future wireless communication system design (Invited Paper),” IEEE Transactions on Communications, vol. 63, no. 9, pp. 3029–3056, Sep. 2015.
13. M. K. Samimi and T. S. Rappaport, “3-D millimeter-wave statistical channel model for 5G wireless system design,” IEEE Transactions on Microwave Theory and Techniques, vol. 64, no. 7, pp. 2207–2225, July 2016.
14. “Local multipath model parameters for generating 5G millimeterwave 3GPP-like channel impulse response,” the 10th Euopean Conference on Antennas and Propagation (EuCAP 2016), April 2016.
15. S. Sun et al., “Investigation of prediction accuracy, sensitivity, and parameter stability of large-scale propagation path loss models for 5G wireless communications,” IEEE Transactions on Vehicular Technology, vol. 65, no. 5, pp. 2843–2860, May 2016.

16. "Synthesizing omnidirectional antenna patterns, received power andpathlossfromdirectionalantennasfor5Gmillimeter-wavecommunications,"in2015IEEEGlobalCommunicationsConference(GLOBECOM), Dec. 2015, pp. 1–7.
17. G. R. MacCartney, Jr. et al., "Indoor office wideband millimeter-wave propagation measurements and channel models at 28 and 73 GHz for ultra-dense 5G wireless networks," IEEE Access, vol. 3, pp. 2388–2424, Oct. 2015.
18. "Millimeter wave wireless communications: New results for rural connectivity," in All Things Cellular16, in conjunction with ACM MobiCom, Oct. 2016.
19. G. R. MacCartney, Jr. and T. S. Rappaport, "Study on 3GPP rural macrocell path loss models for millimeter wave wireless communications," in 2017 IEEE International Conference on Communications (ICC), May 2017, pp. 1–7.
20. MathWorks. [Online]. Available: https://www.mathworks.com/.
21. R. B. Ertel et al., "Overview of spatial channel models for antenna array communication systems," IEEE Personal Communications, vol. 5, no. 1, pp. 10–22, Feb 1998.
22. S. Sun et al., "MIMO for millimeter-wave wireless communications: beamforming, spatial multiplexing, or both?" IEEE Communications Magazine, vol. 52, no. 12, pp. 110–121, Dec. 2014.
23. H. J. Liebe et al., "Propagation modeling of moist air and suspended water/ice particles at frequencies below 1000 GHz," AGARD Conference Proceedings 542, May 1993.
24. T. S. Rappaport, R. W. Heath, Jr., R. C. Daniels, and J. N. Murdock, Millimeter Wave Wireless Communications. Pearson/Prentice Hall 2015.
25. K. Bullington, "Radio propagation at frequencies above 30 megacycles," Proceedings of the IRE, vol. 35, no. 10, pp. 1122– 1136, Oct. 1947.
26. H. T. Friis, "A note on a simple transmission formula," Proceedings of the IRE, vol. 34, no. 5, pp. 254–256, May 1946.
27. M. Hata, "Empirical formula for propagation loss in land mobile radio services," IEEE Transactions on Vehicular Technology, vol. 29, no. 3, pp. 317–325, Aug 1980.
28. J. B. Andersen, T. S. Rappaport, and S. Yoshida, "Propagation measurements and models for wireless communications channels," IEEE Communications Magazine, vol. 33, no. 1, pp. 42–49, Jan 1995.
29. "Investigation of prediction accuracy, sensitivity, and parameter stability of large-scale propagation path loss models from 500 MHz to 100 GHz." [Online]. Available: http://wireless.engineering.nyu.edu/presentations/NTIApropagation-presentation-JUNE-15-2016 v1-3.pdf
30. P. Kyosti et al., "WINNER II channel models," European Commission, IST-WINNER, Tech. Rep. D1.1.2.
31. 3GPP, "Technical specification group radio access network; study on 3d channel model for lte (release 12)," 3rd Generation Partnership Project (3GPP), TR 36.873 V12.2.0, June 2015. [Online]. Available: http://www.3gpp.org/dynareport/36873.htm
32. "Study on channel model for frequency spectrum above 6 GHz," 3rd Generation Partnership Project (3GPP), TR 38.900V14.2.0, Dec. 2016. [Online]. Available: http://www.3gpp.org/DynaReport/38900.htm
33. B. Thoma et al., "Simulation of bit error performance and outage probability of pi/4 DQPSK in frequency-selective indoor radio channels using a measurement-based channel model," in IEEE Global Telecommunications Conference (GLOBECOM), Dec 1992, pp. 1825–1829 vol.3.
34. Q. H. Abbasi et al., "Condition number variability of ultra wideband MIMO on body channels," in 2016 International Workshop on Antenna Technology (iWAT), Feb 2016, pp. 167–169.
35. R. W. Heath and D. J. Love, "Multimode antenna selection for spatial multiplexing systems with linear receivers," IEEE Transactions on Signal Processing, vol. 53, no. 8, pp. 3042–3056, Aug 2005.
36. X. Lu et al., "An improved semi-orthogonal user selection algorithm based on condition number for multiuser MIMO systems," China Communications, vol. 11, no. 13, pp. 23–30, Supplement 2014.
37. N. Bourbaki, Elements of Mathematics, Algebra I. Hermann 1974.
38. M. Matthaiou et al., "Reduced complexity detection for ricean MIMO channels based on condition number thresholding," in 2008 International Wireless Communications and Mobile Computing Conference, Aug 2008, pp. 988–993.
39. A. Adhikary et al., "Joint spatial division and multiplexing for mmwave channels," IEEE Journal on Selected Areas in Communications, vol. 32, no. 6, pp. 1239–1255, June 2014.
40. O. E. Ayach et al., "Spatially sparse precoding in millimeter wave MIMO systems," IEEE Transactions on Wireless Communications, vol. 13, no. 3, pp. 1499–1513, March 2014.
41. Shu Sun et al., " A Novel Millimeter-Wave Channel Simulator and Applications for 5G Wireless Communications" 2017 IEEE international conference on communications (ICC) May 2017.